Pseudo Affine Wigner Distributions: Definition and Kernel Formulation

Paulo Gonçalvès, *Member, IEEE*, and Richard G. Baraniuk, *Senior Member, IEEE*

***Abstract*— In this paper, we introduce a new set of tools for time-varying spectral analysis: the pseudo affine Wigner distributions. Based on the affine Wigner distributions of J. and P. Bertrand, these new time-scale distributions support efficient on-line operation at the same computational cost as the continuous wavelet transform. Moreover, they take advantage of the proportional bandwidth smoothing inherent in the sliding structure of their implementation to suppress cumbersome interference components. To formalize their place within the echelon of the affine class of time-scale distributions (TSD's), we introduce and study an alternative set of generators for this class.**

***Index Terms*— Affine Wigner distributions, time-frequency analysis, wavelets.**

I. Introduction

TIME-VARYING spectral representations, which analyze signals in terms of joint time and frequency coordinates, have proven useful in a wide variety of fields. Most representations of current interest belong to either (or both of) Cohen's class [1] or the affine class [2], [3]. The time–frequency distributions (TFD's) of Cohen's class are covariant to time and frequency shifts of the signal. Classical TFD's such as the spectrogram, Wigner distribution, and pseudo Wigner distribution have been applied to the analysis of narrowband radar, communications, and locally harmonic signals. The time-scale distributions (TSD's, also called *affine time–frequency distributions*) of the affine class, in contrast, are covariant to time shifts and scale changes of the signal. This property makes TSD's natural for applications such as wideband radar and sonar and self-similar signal analysis.

The simplest time-scale representation is the continuous *wavelet transform*. It has the advantage of being a linear expansion of the signal onto a set of analyzing functions, yet its very linearity precludes desirable theoretical properties such as correct marginal distributions and perfect localization. To illustrate the resolution limitations of the wavelet transform, in Fig. 1(a), we plot its squared magnitude (referred to as the scalogram) for a simple test signal.

The quadratic *affine Wigner distributions* proposed in [2] are high-resolution alternatives to the wavelet transform. They have many desirable theoretical properties but, unfortunately, two primary drawbacks as well. First, their bilinearity results in copious interference terms in the time–frequency plane [see Fig. 1(b)] [4], [5]. Second, due to their complicated formulation, efficient implementations suitable for long time series have not been developed for most of these TSD's. As a result, few affine Wigner distributions have been employed in real-world applications.

In this paper, we attack both of these limitations simultaneously by introducing a set of (smoothed) *pseudo affine Wigner distributions*. Like the pseudo Wigner TFD, these new TSD's are based on a short-time window that not only controls the tradeoff between localization and interference attenuation but also provides an efficient on-line computational algorithm. The pseudo affine Wigner distributions permit a continuous transition between the interference-free scalogram and the high-resolution affine Wigner distributions and, thus, should open up new application areas to these powerful tools [see Fig. 1(c) and (d)].

After reviewing the background of TFD's and TSD's in Section II, we derive the pseudo and smoothed pseudo affine Wigner distributions in Section III. In Section IV, we consider their place within the echelon of the affine class of TSD's. The usual formulation of the affine class, as the affine correlation of the Wigner distribution with a kernel function [3], turns out to be inappropriate for studying the pseudo affine Wigner distributions. We will see that a more natural way of proceeding is to replace the Wigner distribution in this formulation with a set of canonical generating TSD's. We close in Section V with a discussion and conclusions.

II. Background on Time–Frequency and Time-Scale Analysis

In this section, we briefly review the elements of the theory of TFD's and TSD's that we will employ in the sequel. TFD's and TSD's are two-dimensional (2-D) functions of time t and frequency f that indicate how the frequency content of a signal x changes over time. Our distinction between TFD's and TSD's stems from their covariance properties: TFD's are covariant to time and frequency shifts, whereas TSD's are covariant to time shifts and scale changes.

A. Time–Frequency Analysis with the Wigner Distribution

1) Wigner Distribution: A TFD C_x of a signal x is *time–frequency shift covariant* if time shifts and modulations

Manuscript received May 4, 1996; revised June 18, 1997. This work was supported by the National Science Foundation under Grant MIP-9457438 and the Office of Naval Research under Grant N00014-95-1-0849. The associate editor coordinating the review of this paper and approving it for publication was Dr. Nurgun Erdol.

P. Gonçalvès is with INRIA Rocquencourt, Le Chesnay, France (e-mail: Paulo.Goncalves@inria.fr).

R. G. Baraniuk is with the Department of Electrical and Computer Engineering, Rice University, Houston, TX 77005-1892 USA (e-mail: richb@rice.edu).

Publisher Item Identifier S 1053-587X(98)03913-0.

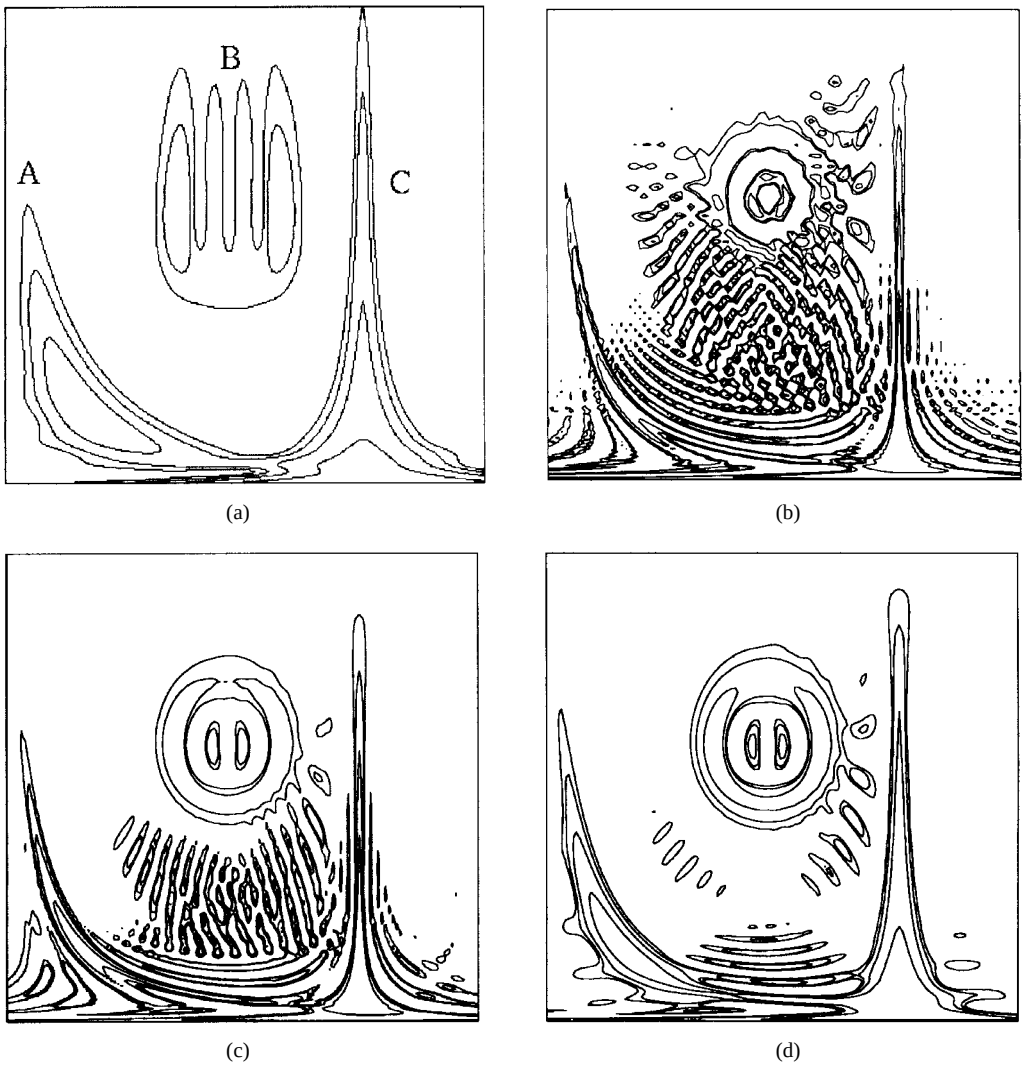

Fig. 1. Time-scale distributions (TSD's) of a test signal composed of a hyperbolic chirp $X_{\mathrm{A}}(f) = e^{i2\pi\alpha \ln f}$ (component A), a third-order Hermite function (component B), and a Lipschitz singularity $x_{\mathrm{C}}(t) = |t - t_0|^{-0.1}$ (component C). TSD's are plotted in equal-energy contours with the horizontal axis corresponding to time and the vertical axis corresponding to frequency. (a) The scalogram (squared magnitude of the wavelet transform $D_x(t, f)$) computed using a Morlet wavelet ψ of quality factor $Q = 2$. (b) Unitary Bertrand distribution $P_x^{(0)}(t, f)$. (c) Pseudo Bertrand distribution $\widetilde{P}_x^{(0)}(t, f)$ computed using a Morlet wavelet of $Q = 8$. (d) Smoothed pseudo Bertrand distribution computed using the same wavelet and a Gaussian frequency window G of $Q = 1$. The pseudo and smoothed pseudo Bertrand distributions permit a continuous transition between the (low-resolution but interference-free) scalogram and the (high-resolution but interference-ridden) Bertrand distribution.

of x result in translations of C_x

$$\begin{array}{ccc} x(t) & \longrightarrow & x(t-t_0)\,e^{i2\pi f_0 t} \\ \downarrow & & \downarrow \\ C_x(t,\ f) & \longrightarrow & C_x(t-t_0,\ f-f_0). \end{array} \tag{1}$$

The simplest TFD is the *spectrogram*, which is the squared magnitude of the short-time Fourier transform[1]

$$S_x(t,f) \equiv \int x(\tau)\, w^*(\tau - t)\, e^{-i2\pi f\tau}\, d\tau. \tag{2}$$

The classical time–frequency resolution tradeoff of the spectrogram, which is controlled by the analysis window w, has prompted the development of more advanced bilinear TFD's, including the *Wigner distribution* [1], [6]

$$W_x(t,f) \equiv \int x\Big(t+\frac{\tau}{2}\Big)x^*\Big(t-\frac{\tau}{2}\Big)e^{-i2\pi f\tau}\, d\tau \tag{3}$$

$$= \int X\Big(f+\frac{\nu}{2}\Big)X^*\Big(f-\frac{\nu}{2}\Big)e^{i2\pi\nu t}\, d\nu. \tag{4}$$

This TFD can be interpreted as a short-time Fourier transform with the window matched to the signal. In addition to time–frequency shift covariance, the Wigner distribution supports additional covariances to scale changes and to linear chirp modulations and convolutions [1], [6].

2) Pseudo Wigner Distribution: Although the Wigner distribution has many desirable properties, it also has two major limitations. First, it does not support on-line operation, since its calculation requires the entire signal. Second, its interpretation is complicated by nonlinear interference components [1],

[1]Unless specified, bounds of integration run from $-\infty$ to $+\infty$. In this paper, we will consider only analytic signals for which $X(f) \equiv 0\ \forall f < 0$, with X the Fourier transform of the time signal x.

[6]. The *pseudo Wigner distribution* tackles both limitations simultaneously.

The pseudo Wigner distribution [7] is a sliding version of the Wigner distribution obtained by inserting a window function h into (3)

$$\widetilde{W}_x(t,f) \equiv \int h(\tau)\, x\left(t+\frac{\tau}{2}\right) x^*\left(t-\frac{\tau}{2}\right) e^{-i2\pi f\tau}\, d\tau. \quad (5)$$

Loosely speaking, this TFD is equivalent to the Wigner distribution of the time windowed signal $x(\tau)\sqrt{h(2\tau-t)}$, meaning that large amounts of data can be treated online. Stankovic has noted that the pseudo Wigner distribution can also be written as the "matched-filter" correlation of the short-time Fourier transform [using window $w(\tau)=\sqrt{h(2\tau)}$] with itself [8]

$$\widetilde{W}_x(t,f) = \int S_x\left(t, f+\frac{\nu}{2}\right) S_x^*\left(t, f-\frac{\nu}{2}\right) e^{i2\pi\nu t}\, d\nu. \quad (6)$$

This formula echoes the structure of (4) with the Fourier transform of the signal simply replaced by its short-time Fourier transform. Thus, we can identify the pseudo Wigner distribution as one of the two fundamental bilinear TFD's derived from the short-time Fourier transform:

> The spectrogram results from squaring the short-time Fourier transform; the pseudo Wigner distribution results from a self-correlation of the short-time Fourier transform across frequency.

The time windowing in (5) acts as a smoothing in the frequency domain; therefore, the pseudo Wigner distribution suppresses the Wigner distribution interference components that oscillate in the frequency direction. Time direction smoothing can be implemented by convolving (5) with a lowpass function q

$$\widetilde{W}_x(t,f) \equiv \int q(u-t) \int h(\tau)\, x\left(u+\frac{\tau}{2}\right) x^*\left(u-\frac{\tau}{2}\right) \times e^{-i2\pi f\tau}\, d\tau\, du. \quad (7)$$

The result is known as the *smoothed pseudo Wigner distribution*.[2] An alternative approach to time smoothing limits the range of the integral in (6) with a lowpass function G [8]

$$\widetilde{W}_x(t,f) = \int G(\nu)\, S_x\left(t, f+\frac{\nu}{2}\right) S_x^*\left(t, f-\frac{\nu}{2}\right) e^{i2\pi\nu t}\, d\nu. \quad (8)$$

Note that the TFD's (7) and (8) are not equivalent in general.

3) Cohen's Class: The spectrogram, Wigner distribution, (smoothed) pseudo Wigner distribution, and all other time–frequency shift covariant TFD's belong to *Cohen's class* of TFD's. The Wigner distribution can be interpreted as the central, generating member of this class, with each Cohen's class TFD C obtained via the 2-D correlation [1]

$$C_x(t,f) = \iint W_x(\tau,\nu)\, \Pi(\tau-t, \nu-f)\, d\tau\, d\nu \quad (9)$$

with Π the *kernel* of C. The spectrogram kernel is the Wigner distribution of the analysis window itself: $\Pi_{\mathrm{spec}}(t,f) = W_w(t,f)$. The kernel corresponding to the smoothed pseudo Wigner distribution (7) is the separable form $\Pi_{\mathrm{spwd}}(t,f) = q(t)\, H(f)$. The kernel for the Stankovic smoothed pseudo Wigner distribution (8) is

$$\Pi_{\mathrm{Sspwd}}(t,f) = g(t)\, W_w(t,f) \quad (10)$$

meaning that this TFD strikes a balance in smoothing between the pseudo Wigner distribution $[g(t)=\delta(t)]$ and the spectrogram $[g(t)=1]$.

B. Time-Scale Analysis with the Affine Wigner Distributions

1) Affine Wigner Distributions: A TSD Ω_x of a signal x is *time-scale covariant*, or *affine covariant*, if time shifts and scale changes of x result in translations and scale changes of Ω_x [2], [3]

$$\begin{array}{ccc} x(t) & \longrightarrow & \frac{1}{\sqrt{\alpha}}\, x\left(\frac{t-t_0}{\alpha}\right) \\ \downarrow & & \downarrow \\ \Omega_x(t,f) & \longrightarrow & \Omega_x\left(\frac{t-t_0}{\alpha}, \alpha f\right). \end{array} \quad (11)$$

Like a TFD, a TSD measures the joint time–frequency content of a signal. We use the terminology TSD/TFD merely to differentiate the time-scale covariance of affine class distributions from the time–frequency shift covariance of Cohen's class distributions.

The simplest TSD is the *scalogram*, which is the squared magnitude of the continuous wavelet transform [3][3]

$$\begin{aligned} D_x(t,f) &\equiv f^{1/2} \int x(\tau)\, \psi^*[f(\tau-t)]\, d\tau \\ &= f^{-1/2} \int_0^\infty X(\nu)\, \Psi^*(\nu/f)\, e^{i2\pi\nu t}\, d\nu. \end{aligned} \quad (12)$$

The scalogram has a proportional-bandwidth time–frequency resolution tradeoff[4] controlled by the analysis wavelet ψ that parallels that of the spectrogram [3]. This limitation prompted the development of more advanced bilinear TSD's, including the *affine Wigner distributions* of J. and P. Bertrand [2], [9].

There are an infinite number of affine Wigner distributions, each labeled by an index $k \in \mathbb{R}$. The kth affine Wigner distribution of an analytic signal x is defined in terms of its Fourier transform X as [2]

$$\begin{aligned} P_x^{(k)}(t,f) \equiv f \int & X[\lambda_k(u) f]\, X^*[\lambda_k(-u) f] \\ & \times\ e^{i2\pi t f \xi_k(u)}\, \mu_k(u)\, du, \quad f>0 \end{aligned} \quad (13)$$

with $\mu_k(u)$ an arbitrary positive, continuous function, and

$$\lambda_k(u) = \left(k\,\frac{e^{-u}-1}{e^{-ku}-1}\right)^{1/(k-1)}, \quad k \neq 0,1 \quad (14)$$

$$\xi_k(u) = \lambda_k(u) - \lambda_k(-u). \quad (15)$$

[2] We will abuse notation and employ the same tilde symbol (as in $\widetilde{W}_x$) to denote all "pseudo" distributions. The particular form in use will be clear from context.

[3] Usually, the wavelet transform is expressed as a function of a time variable t and a scale variable a. Here, we will use the reparameterization of scale as inverse frequency $a = f_0/f$ suggested in [3] and assume without loss of generality that the center frequency f_0 of the wavelet ψ equals 1 Hz.

[4] Equivalently, *constant-Q*, with the Q factor defined as analysis frequency over analysis bandwidth.

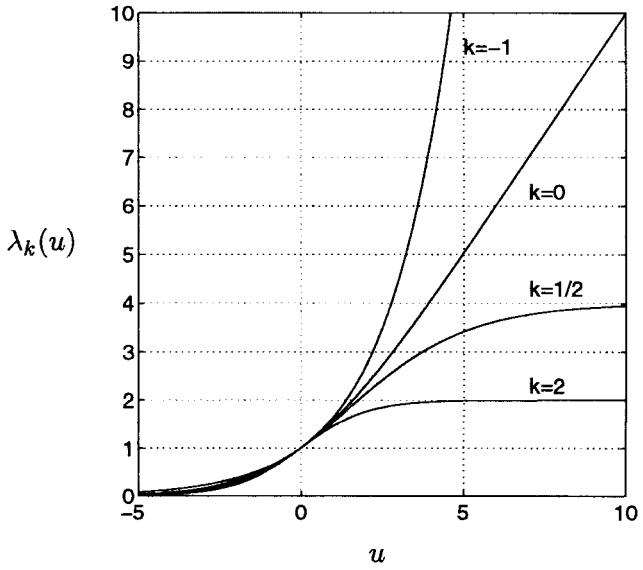

Fig. 2. Graphs of the function $\lambda_k(u)$ versus u for various values of the index k.

Taking limits as $k \to 0, 1$, we obtain

$$\lambda_0(u) = \frac{u}{1 - e^{-u}}, \qquad \lambda_1(u) = \exp\left(1 + \frac{u\,e^{-u}}{e^{-u} - 1}\right). \quad (16)$$

Fig. 2 illustrates the behavior of the λ_k function. This function has the symmetry property

$$\lambda_k(-u) = e^{-u}\,\lambda_k(u). \quad (17)$$

In addition to time-scale covariance, each affine Wigner distribution $P^{(k)}$ has a third, "extended" covariance to transformations along a power-law (or logarithmic) group delay matched to the index k

$$\begin{array}{ccc} X(f) & \longrightarrow & e^{-i2\pi\Phi_k(f)}\,X(f) \\ \downarrow & & \downarrow \\ P_x^{(k)}(t,f) & \longrightarrow & P_x^{(k)}\left[t - \dfrac{d}{df}\Phi_k(f), f\right]. \end{array} \quad (18)$$

The phase spectra take different forms depending on k

$$\begin{array}{ll} k \neq 0, 1 & \Phi_k(f) = cL_k f^k \\ k = 0 & \Phi_0(f) = c(L_0 + \kappa d_0 \ln f) \\ k = 1 & \Phi_1(f) = cf(L_1 + \ln f) \end{array} \quad (19)$$

with c, d_0, κ, and L_k real constants (see [2] for details). As a result, the index k controls the geometry of the affine Wigner distributions [4], [5]. The function μ_k controls the localization, marginal, and unitarity[5] properties of $P^{(k)}$. (Note that since μ_k is arbitrary, for each k, there are infinitely many different $P^{(k)}$ TSD's.)

Several classical TSD's live within the affine Wigner framework:

1) $k = 2$—*Wigner Distribution:* In this case, $\lambda_2(u) = 1 + \tanh(u/2)$ and $\xi_2(u) = 2\tanh(u/2)$. This choice results in TSD's with extended covariance along straight line paths $t = (d/df)\Phi_2(f) \propto f$ in the time–frequency plane.

   More specifically, choosing $\mu_2(u) = [\lambda_2(u)\lambda_2(-u)(d/du)\xi_2(u)]^{1/2} = 1 - \tanh^2(u/2)$ yields the Wigner distribution (4) (for analytic signals). This particular $P^{(2)}$ TSD is unitary and satisfies the time, frequency, and linear chirp marginals.

2) $k = 1/2$—*D-Distribution:* In this case, $\lambda_{(1/2)}(u) = [1 + \tanh(u/4)]^2$ and $\xi_{(1/2)}(u) = 4\tanh(u/4)$. This choice results in TSD's with extended covariance along square-root-hyperbolic paths $t = (d/df)\Phi_{1/2}(f) \propto f^{-1/2}$ in the time–frequency plane.

   Choosing $\mu_{1/2}(u) = 1 - \tanh^2(u/4)$ yields the D-distribution of Flandrin [4], [5], [10].

3) $k = 0$—*Bertrand Distribution:* In this case, $\lambda_0(u) = -u/(e^{-u} - 1)$ and $\xi_0(u) = u$. This choice results in TSD's with extended covariance along hyperbolic time–frequency paths $t = (d/df)\Phi_0(f) \propto f^{-1}$.

   Choosing $\mu_0(u) = [\lambda_0(u)\lambda_0(-u)]^{1/2}$ yields the unitary Bertrand distribution [9], [11]

$$P_x^{(0)}(t,f) \equiv f \int \frac{u}{2\sinh(u/2)}\,X\left[\frac{fue^{u/2}}{2\sinh(u/2)}\right] \times\, X^*\left[\frac{fue^{-u/2}}{2\sinh(u/2)}\right] e^{i2\pi tfu}\,du. \quad (20)$$

   This particular $P^{(0)}$ TSD is unitary and localizes in time and along hyperbolic group delays. It marginalizes to frequency when integrated over time and to the Mellin transform [2], [6] when integrated along hyperbolic paths $tf = c$.

4) $k = -1$—*Unterberger Distribution:* In this case, $\lambda_{-1}(u) = e^{u/2}$ and $\xi_{-1}(u) = 2\sinh(u/2)$. This choice results in TSD's with extended covariance along time–frequency paths of the form $t = (d/df)\Phi_{-1}(f) \propto f^{-2}$.

   Choosing $\mu_{-1}(u) = \cosh(u/2)$ yields the active Unterberger distribution [4], [5], [12]

$$\begin{aligned} P_x^{(-1)}(t,f) &\equiv f \int \cosh\left(\frac{u}{2}\right) X\left(e^{u/2} f\right) X^*\left(e^{-(u/2)} f\right) \\ &\quad \times e^{i4\pi tf\sinh(u/2)}\,du \\ &= f \int \left(1 + \frac{1}{\gamma^2}\right) X(\gamma f)\,X^*\left(\frac{1}{\gamma} f\right) \\ &\quad \times e^{i2\pi tf[\gamma - (1/\gamma)]}\,d\gamma. \end{aligned} \quad (21)$$

   This TSD localizes in time and along hyperbolic square group delays and satisfies the frequency marginal.

5) $k = \pm\infty$—*Margenau–Hill Distribution:* The Margenau–Hill distribution [1], [2] arises as the arithmetic mean of the distributions $P^{(\infty)}$ and $P^{(-\infty)}$ parameterized by

$$\lambda_+(u) = \lim_{k \to +\infty} \lambda_k(u) = U(u) + e^u\,U(-u) \quad (22)$$

$$\lambda_-(u) = \lim_{k \to -\infty} \lambda_k(u) = U(-u) + e^u\,U(u) \quad (23)$$

$$\xi_\pm(u) = e^{\pm|u|} \quad (24)$$

[5] A distribution P is unitary if $|\int x(t)\,y^*(t)\,dt|^2 = \iint P_x(t,f)\,P_y(t,f)\,dt\,df$.

with U the Heaviside unit step function. This TSD is time localized and has correct time and frequency marginals.

In addition to these examples, there exist an infinite number of unexplored affine Wigner distributions of other orders k. Currently, most of these distributions are hardly accessible, however, due to a lack of simple algorithms for their computation.

2) Affine Class: The scalogram, the affine Wigner distributions, and all other bilinear time-scale covariant distributions belong to the *affine class* of TSD's. As in Cohen's class, the Wigner distribution $W = P^{(2)}$ is usually taken as the central generating member of this class, with each affine TSD Ω obtained via the 2-D affine correlation [3]

$$\Omega_x(t,f) = \iint_0^\infty W_x(\tau,\nu)\, \Pi\left[f(\tau-t),\, \frac{\nu}{f}\right] d\nu\, d\tau \qquad (25)$$

with Π the kernel of Ω. The scalogram kernel is the Wigner distribution of the analysis wavelet ψ: $\Pi_{\text{scalo}} = W_\psi$ [3], [13].

III. Pseudo Affine Wigner Distributions

The affine Wigner distributions (13) have great potential as flexible tools for time-varying spectral analysis. They possess a number of desirable theoretical properties, including the ability to match a large class of different signal types. Unfortunately, their promise is offset by two major practical limitations. First, the entire signal enters into the calculation of these TSD's at every point $(t,\, f)$ in the time–frequency plane, precluding their on-line operation with long signals. Second, due to their nonlinearity, interference components arise between each pair of signal components, complicating their interpretation (recall Fig. 1) [4], [5]. As a result, few affine Wigner distributions have been applied in practice (aside from in [14]).

In this section, we attack these limitations by introducing a set of (smoothed) *pseudo affine Wigner distributions* [15]. These new TSD's offer not only asymptotically the same properties as the affine Wigner distributions but also support efficient on-line operation and suppress troublesome interference components. Our derivation relies on the strong analogy between time–frequency and time-scale analysis and is inspired by the pseudo Wigner distribution.

A. Derivation

Recall from Section II-A that we obtain the pseudo Wigner distribution (5) by introducing a window function into the Wigner distribution (3). An analogous windowing procedure leads to the pseudo affine Wigner distributions. In contrast to the pseudo Wigner case, however, this windowing must be frequency-dependent to ensure that the resulting TSD remains affine covariant.[6] As a result, the smoothing in frequency direction is proportional bandwidth, rather than constant-bandwidth as in the pseudo Wigner distribution.

We first rewrite the general form (13) in the time domain

$$P_x^{(k)}(t,f) = f \int \mu_k(u) \left[\int x(\tau)\, e^{-i2\pi\lambda_k(u) f(\tau-t)}\, d\tau\right] \times \left[\int x(\tau')\, e^{-i2\pi\lambda_k(-u) f(\tau'-t)}\, d\tau'\right]^* du. \qquad (26)$$

It is clear from this expression that at every point $(t,\, f)$ in the time–frequency plane, the affine Wigner distribution depends on the entire signal x. Since on-line operation requires that we consider the signal only in a sliding interval, we introduce a window function h in (26) to obtain

$$\begin{aligned}\widetilde{P}_x^{(k)}(t,f) &\equiv f \int \mu_k(u) \left[\int x(\tau) h[f\lambda_k(u)(\tau-t)] e^{-i2\pi\lambda_k(u) f(\tau-t)} d\tau\right] \\ &\quad \times \left[\int x(\tau')\, h[f\lambda_k(-u)(\tau'-t)]\, e^{-i2\pi\lambda_k(-u) f(\tau'-t)}\, d\tau'\right]^* \\ &\quad \times du. \end{aligned} \qquad (27)$$

The dependence of h on the analysis frequency f guarantees $\widetilde{P}^{(k)}$ affine covariance to time shifts and scale changes.[7] By analogy to the pseudo Wigner distribution, we call these new TSD's *pseudo affine Wigner distributions*.

The pseudo affine Wigner distributions can be formulated in terms of the wavelet transform. Introducing the bandpass wavelet function $\psi(\tau) = h(\tau)\, e^{i2\pi\tau}$, we can reorder (27) as

$$\begin{aligned}\widetilde{P}_x^{(k)}(t,f) &= f \int \mu_k(u) \left[\int x(\tau)\, \psi^*[f\lambda_k(u)(\tau-t)]\, d\tau\right] \\ &\quad \times \left[\int x(\tau')\, \psi^*[f\lambda_k(-u)(\tau'-t)]\, d\tau'\right]^* du \\ &= \int \frac{\mu_k(u)}{\sqrt{\lambda_k(u)\lambda_k(-u)}}\, D_x[t,\, \lambda_k(u) f] \\ &\quad \times D_x^*[t,\, \lambda_k(-u) f]\, du \end{aligned} \qquad (28)$$

with D_x the wavelet transform (12) computed with wavelet ψ. This generalized "matched filter" correlation of the wavelet transform with itself echoes the structure of (13) with the Fourier transform of the signal X replaced by its wavelet transform D_x. It also parallels the expression (6) that holds for the short-time Fourier transform and pseudo Wigner distribution. Thus, we can identify the pseudo affine Wigner distribution as one of the two fundamental bilinear TSD's derived from the wavelet transform:

> The scalogram results from squaring the wavelet transform; the pseudo affine Wigner distribution results from a generalized self-correlation of the wavelet transform across frequency.

Fig. 3 illustrates the focusing effect of the generalized self-correlation (28) on a time slice of the wavelet transform. To compute the self-correlation at frequency f, we scale and warp $D_x(t,f)$ to the function $D_x[t,\, \lambda_k(u) f]$ and then compute the inner product over u between this function and its reversed twin $D_x^*[t,\, \lambda_k(-u) f]$. In contrast with a simple affine

[6] Rioul and Flandrin consider the same covariance requirements in their definition of the affine pseudo Wigner distribution [3]. In this paper, we generalize their definition to the entire class of affine Wigner distributions.

[7] Suppressing the $\lambda_k(\pm u)$ factors in h in (27) yields a different distribution with similar covariance properties. However, this formulation does not appear to admit an efficient implementation.

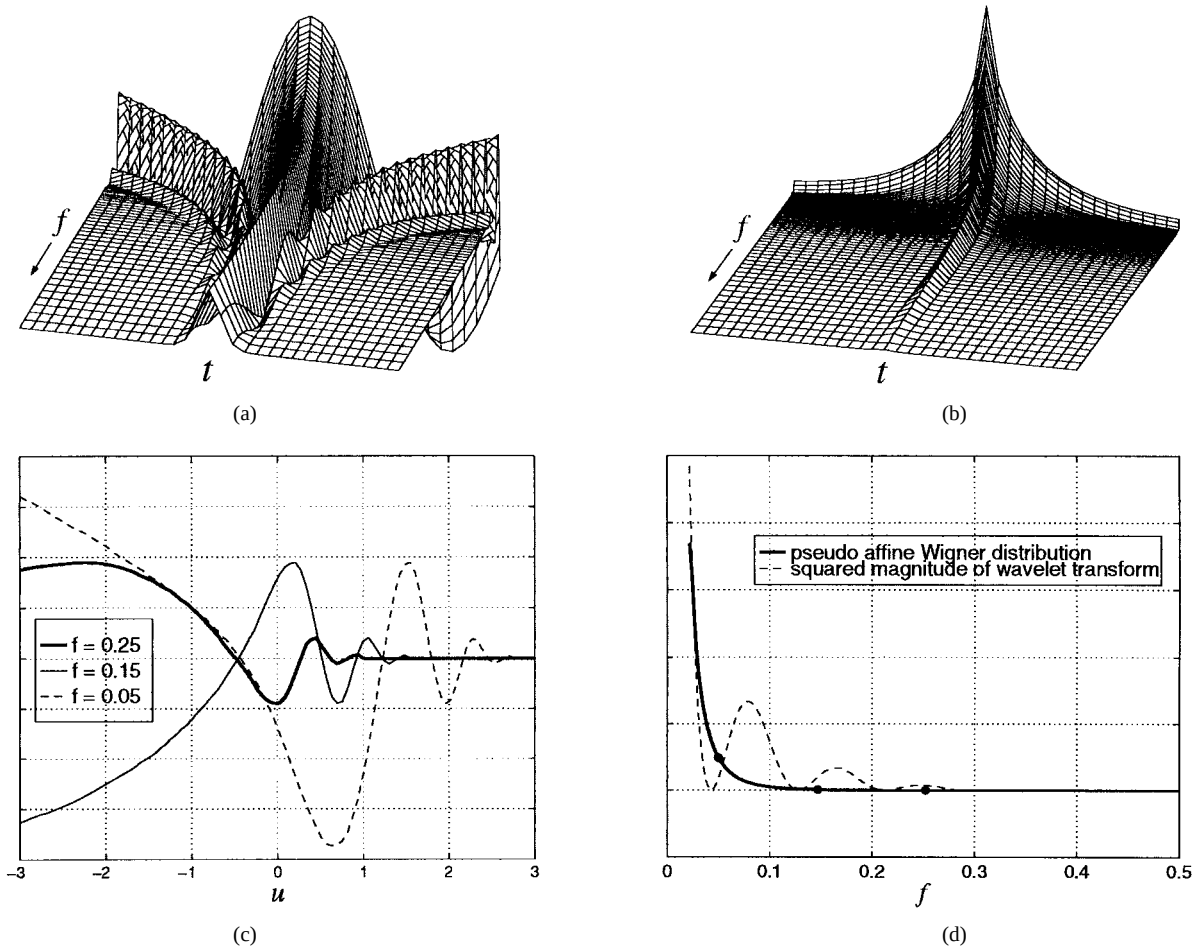

Fig. 3. Computation of the pseudo affine Wigner distribution from the wavelet transform, emphasizing the focusing effect of the generalized matched correlation underlying (28). (a) Wavelet transform (real part) $D_x(t, f)$ of the singularity (component C) from Fig. 1. (Note that the frequency axis runs from top to bottom in this mesh plot.) (b) Pseudo affine Wigner distribution $\widetilde{P}_x^{(0)}(t, f)$ of the same signal. Consider the computation (28) of a time slice $\widetilde{P}_x^{(0)}(t_1, f)$ of this distribution in the vicinity of the singularity. (c) Scaled and warped wavelet transform $D_x[t_1, \lambda_0(u)f]$ plotted versus u for $f = 0.25$, $f = 0.15$, and $f = 0.05$. (d) Result of the generalized matched correlation $\widetilde{P}_x^{(0)}(t_1, f)$ compared with the corresponding time slice of the scalogram $|D_x(t_1, f)|^2$.

correlation, the function is not only scaled but also reshaped before computing the inner product.

B. Time–Frequency Smoothing Interpretation

The time windowing introduced in (27) acts as a proportional bandwidth frequency smoothing that suppresses interference components oscillating in the frequency direction. Compare, for example, the pseudo Bertrand distribution $\widetilde{P}^{(0)}$ of Fig. 1(c) with the unitary Bertrand distribution $P^{(0)}$ of Fig. 1(b).

To suppress interference terms oscillating in the time direction, we must smooth in that direction [as in (7)] or window the dual variable [as in (8)]. The introduction of a lowpass function G in (28) limits the integration with respect to u (loosely speaking, the dual variable of the product tf), and thus performs proportional-bandwidth time smoothing of the TSD. We call the resulting time-scale distributions

$$\widetilde{P}_x^{(k)}(t, f) = \int G(u) \frac{\mu_k(u)}{\sqrt{\lambda_k(u)\lambda_k(-u)}} D_x[t, \lambda_k(u)f] \times D_x^*[t, \lambda_k(-u)f]\, du \quad (29)$$

the *smoothed pseudo affine Wigner distributions* [see Fig. 1(d)].

Even though the pseudo and smoothed pseudo affine Wigner distributions are smoothed versions of the affine Wigner distributions, they can still have resolution exceeding that of the scalogram [recall Fig. 1(a)]. This resolution enhancement compared with the scalogram is due precisely to the action of the generalized self-correlation in (29); rather than simply squaring the wavelet transform, we match-filter it.

C. Implementation

The pseudo affine Wigner distributions can be interpreted as sliding versions of the original affine Wigner distributions, and as a result, they are naturally suited for on-line operation with long signals. To construct a pseudo affine Wigner distribution, we simply compute the wavelet transform of the signal and then, at each time point, perform the generalized frequency correlation (28) or (29). The fast Mellin transform is a convenient tool for implementing this correlation efficiently [16], [17]. The algorithm runs as follows:[8]

[8]Matlab code for computing the smoothed pseudo affine Wigner distributions is available from Rice University DSP home page at www.dsp.rice.edu and INRIA at www.syntim.inria.fr/fractales/software/TFTB/.

1) Compute the wavelet transform $D_x(t,f)$ of the signal using wavelet $\psi(\tau) = h(\tau)\, e^{i2\pi\tau}$. Samples should be spaced uniformly in time and exponentially in frequency.
2) At each time t, for a range of u, rescale $D_x(t,f)$ to $D_x[t, \lambda(\pm u)f]$ using the Mellin transform [17], which maps scale changes to simple phase shifts. Since the Mellin transform of a function $z(v)$ equals the Fourier transform of $e^{v/2}z(e^v)$, a fast Fourier transform (FFT) applied to an exponentially spaced set of frequency samples of $D_x(t,f)$ implements a fast Mellin transform.
3) At each time t, compute the inner product (28) or (29) with respect to u.

Using a fast algorithm for the computation of the wavelet transform [17], [18], the computational cost of this procedure is $O(MN\log M)$ for N time and M frequency samples,[9] which is on the same order as the cost for the spectrogram, pseudo Wigner distribution, and scalogram.

D. Examples

1) $k = 2$—*Affine Pseudo Wigner Distribution:* In this case, (13) reduces to the ordinary Wigner distribution, and (29) becomes the "affine smoothed pseudo Wigner distribution" of Rioul and Flandrin [3].
2) $k = 0$—*Pseudo Bertrand Distribution:* In the particular case of the unitary $P^{(0)}$ distribution (20), the special form for $\mu_0(u)$ cancels the $\sqrt{\lambda_0(u)\lambda_0(-u)}$ factor in (28), leaving us with a much simpler expression for $\widetilde{P}^{(0)}$. The result is the pseudo Bertrand distribution of [16].

   In Fig. 1, we demonstrated the performance of this new TSD on a synthetic test signal. In Fig. 4, we plot the Wigner, Bertrand, scalogram, and smoothed pseudo Bertrand TSD's of the echo-location chirp of the large brown bat *Eptesicus Fuscus*. The approximate hyperbolic localization of the smoothed pseudo Bertrand distribution matches the chirping nature of the signal, whereas the proportional-bandwidth time–frequency smoothing suppresses the interference components that swamp both the Wigner and Bertrand distributions.
3) $k = -1$—*Pseudo Unterberger Distribution:* Due to their affine covariance properties, TSD's have a unique ability to analyze low frequencies with good frequency resolution and high frequencies with good time resolution. The active Unterberger distribution, furthermore, is time localized and preserves the scaling properties of signal components [19], making it ideal for the study of transients. The primary drawback of this bilinear TSD is the existence of interference components between transient events.

   The pseudo Unterberger distribution smooths interference components in the frequency direction while preserving the correct scaling structure across frequency. In Fig. 5, we compare the performance of this new TSD to the pseudo Wigner TFD and scalogram on a machine fault signature.
4) $k = \pm 5$—*Approximate Affine Wigner Distributions:* Up to this point, we have emphasized the ability of the smoothed pseudo affine Wigner distributions to control interference components through time–frequency smoothing. More generally, however, our approach allows us to efficiently approximate all (unsmoothed) affine Wigner distributions, even for unusual values of the index k for which the algorithm proposed in [17] does not apply directly. In the limit as the bandwidth of the wavelet ψ falls to zero, we have $\widetilde{P}_x^{(k)} \rightarrow P_x^{(k)}$. Therefore, a pseudo affine Wigner distribution (28) computed using a narrowband wavelet will closely approximate its corresponding affine Wigner distribution, including its marginal and extended covariance (18) properties. [In general, a (smoothed) pseudo affine Wigner distribution will not possess all possible theoretical properties of the affine Wigner TSD's; however, we could constrain the choice of the wavelet ψ to preserve certain of them.]

   In approximating an affine Wigner distribution, our goal is not to suppress interference components but rather to *preserve* them. Fig. 6 illustrates the close agreement between the approximate affine Wigner distributions $\widetilde{P}_x^{(-5)}$ and $\widetilde{P}_x^{(5)}$ and the theoretical loci of the true distributions as determined by the geometric construction rules of [4] and [5]. To obtain these TSD's, we employed a narrowband wavelet of $Q = 130$ in (28).

[9] Assuming that the length of the wavelet at maximum dilation is of $O(M)$.

IV. Pseudo Affine Wigner Distributions and the Affine Class

Like all affine Wigner distributions, the pseudo affine Wigner distributions belong to the affine class of TSD's that, as defined in (25), revolves around the Wigner distribution $W = P^{(2)}$. Unfortunately, this formalism becomes awkward when we try to derive an analytic form for the kernel Π corresponding to a pseudo affine Wigner distribution. In this section, we investigate an alternative canonical formulation for the affine class in which the kernels corresponding to the pseudo affine Wigner distributions have an easily identifiable, closed form.

For each $k \in \mathbb{R}$, we will replace W in (25) with an alternative, matched generator TSD $W^{(k)}$ that provides a natural framework for the affine Wigner distributions $P^{(k)}$ and the pseudo affine Wigner distributions $\widetilde{P}^{(k)}$. With this new formalism, all affine class TSD's can be written as

$$\Omega_x(t,f) = \iint_0^\infty W_x^{(k)}(\tau,\nu)\, \Pi\left[f(\tau - t),\, \frac{\nu}{f}\right] d\nu\, d\tau \qquad (30)$$

with a different kernel Π for each choice of generator $W^{(k)}$.

A. Affine Wigner Generators

Any TSD that is continuously invertible (*regular* in the terminology of [20]) can play the role of $W^{(k)}$ in (30). In particular, $W^{(k)}$ does not have to be unitary. For the affine Wigner distributions, Fourier transformation of (13) followed by reparameterization using (15) and (17) leads to

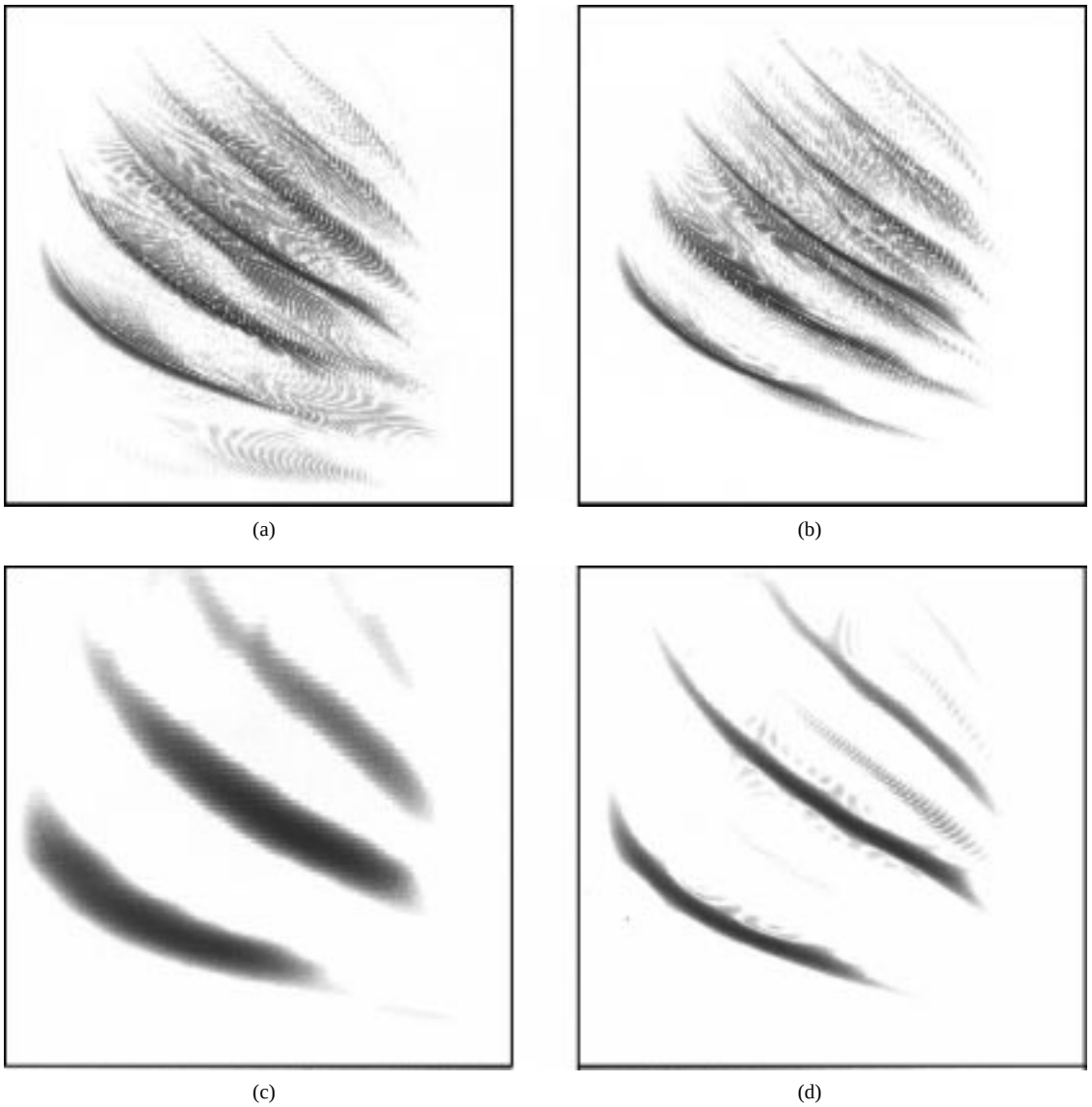

Fig. 4. TSD's of the echo-location chirp of the large brown bat *Eptesicus Fuscus*. Horizontal axis corresponds to time and vertical axis to frequency. (a) Wigner distribution $P_x^{(2)}$. (b) Unitary Bertrand distribution $P_x^{(0)}$. (c) Scalogram $|D_x|^2$. (d) Smoothed pseudo Bertrand distribution $\widetilde{P}_x^{(0)}$.

the inversion formula (for X as a function of u)

$$X(e^u f_0) = \frac{1}{X^*(f_0)} \frac{\frac{d}{du}\xi(u)}{\mu(u)} \int P_x^{(k)}\left[t, \frac{f_0}{\lambda(-u)}\right] \times e^{-i2\pi t f_0(e^u-1)}\, dt \tag{31}$$

with f_0 a constant such that $X(f_0) \neq 0$. This inverse is continuous, provided the term $C(u)$ in front of the integral remains bounded from above and below, with $0 < \epsilon \leq C(u) < \infty$. The affine Wigner distributions thus provide a family of generators for the affine class.

In Appendix A, we single out the affine Wigner generators most natural for studying the pseudo affine Wigner distributions. These generators take the form

$$W_x^{(k)}(t,f) \equiv f \int X[f\lambda_k(u)]\, X^*[f\lambda_k(-u)] \times e^{i2\pi t f \xi_k(u)} \frac{d\xi_k(u)}{du}\, du \tag{32}$$

and correspond to the special choice $\mu_k(u) = (d/du)\xi_k(u)$ in (13).[10] With this generator installed in (30), the kernel corresponding to the (smoothed) pseudo affine Wigner distribution $\widetilde{P}^{(k)}$ can be written in closed form as

$$\Pi^{(k)}(t,f) = f \iint G(u)\mu(u) \frac{\lambda_k(v)\lambda_k(-v)}{\lambda_k(u)\lambda_k(-u)} \times \Psi\left[f\frac{\lambda_k(v)}{\lambda_k(u)}\right] \Psi^*\left[f\frac{\lambda_k(-v)}{\lambda_k(-u)}\right] e^{i2\pi t f \xi_k(v)}\, du\, dv. \tag{33}$$

B. Examples

Each different $k \in \mathbb{R}$ yields a different generator $W^{(k)}$ matched to the specific geometry of the affine Wigner distri-

[10] With $\mu_k(u) = (d/du)\xi_k(u)$, the term $C(u)$ in front of the integral in (31) reduces to a constant.

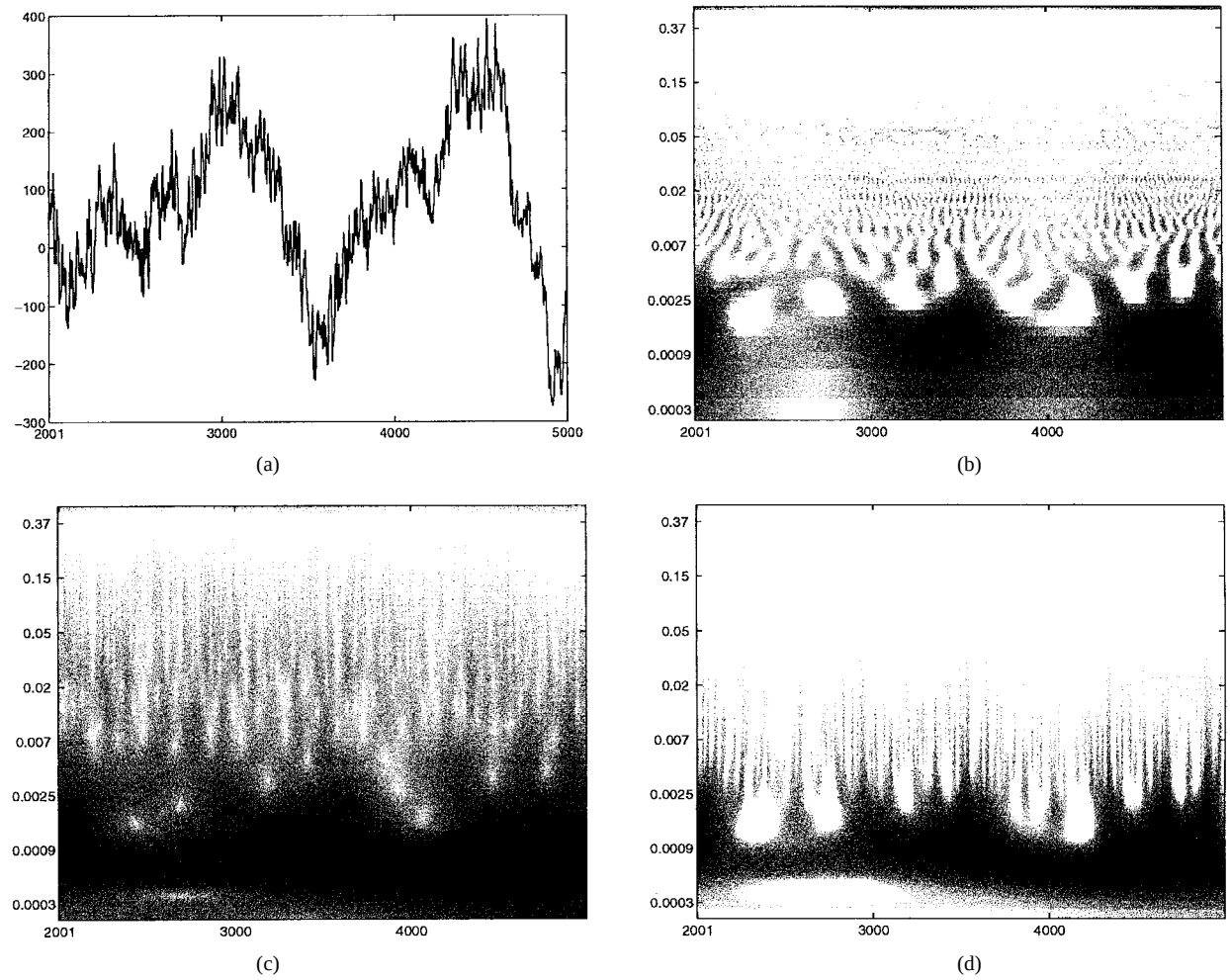

Fig. 5. Time-varying spectral representations in a machine fault monitoring application. (a) Five thousand samples of a time series acquired from an accelerometer axially mounted on a main condensate pump rotating at 892 r/min. The sampling rate was 50 kHz. (b) Pseudo Wigner TFD $\widetilde{W}_x$ computed using a 1024-point sliding window. This Cohen's class TFD is not scale covariant; hence, it cannot reveal both the low-frequency rotational components and the high-frequency transients. (The horizontal axis corresponds to time and the vertical axis to normalized frequency in a logarithmic scale.) (c) Scalogram $|D_x|^2$ computed using a Mexican hat wavelet. This affine class TSD is scale covariant but suffers from low resolution. (d) Pseudo Unterberger distribution $\widetilde{P}_x^{(-1)}$ computed using the same Mexican hat wavelet (and $G \equiv 1$). This TSD localizes both the fundamental rotation frequency and the transient events. (Data taken from the "NRad" test data set courtesy of J. Allen of NCCOSC and D. Lake of the Office of Naval Research.)

butions $P^{(k)}$ and the pseudo affine Wigner distributions $\widetilde{P}^{(k)}$. Examples include the following.

1) $k = 2$—*Wigner Distribution:* Using $\mu_2(u) = (d/du)\xi_2(u) = 1 - \tanh^2(u/2)$ in (13), we retrieve the Wigner distribution (4) and the usual affine class definition (25). The Wigner distribution is the sole unitary generator of the form (32) (see Appendix B for the proof).
2) $k = 0$—*Nonunitary Bertrand Distribution:* Using $\mu_0(u) = (d/du)\xi_0(u) = 1$ in (13), we obtain a (nonunitary) Bertrand distribution.
3) $k = -1$—*Active Unterberger Distribution:* Using $\mu_{-1}(u) = (d/du)\xi_{-1}(u) = \cosh(u/2)$ in (13), we encounter the active form of the Unterberger distribution. This TSD is the sole generator of the form (32) that is time localized according to the definition of [2] (see Appendix C for the proof).

The scalogram has a different representation in terms of each generator. Recall that the unitarity of the Wigner distribution permits us to write the scalogram as an affine correlation of two Wigner distributions [3], [13][11]

$$|D_x(t,f)|^2 = \iint_0^\infty W_x(\tau,\nu)\, W_\psi\Big[f(\tau-t), \frac{\nu}{f}\Big]\, d\nu\, d\tau. \quad (34)$$

This formula generalizes to the generators $W^{(k)}$ of (32). To see this, note that setting $G(u) = \delta(u)$ reduces (29) to the scalogram and (33) to

$$\begin{aligned}\Pi^{(k)}(t,f) &= \widehat{W}_\psi^{(k)}(t,f) \\ &\equiv f\int \lambda_k(v)\,\lambda_k(-v)\,\Psi[f\lambda_k(v)]\,\Psi^*[f\lambda_k(-v)] \\ &\quad \times e^{j2\pi t f \xi_k(v)}\, dv. \end{aligned} \quad (35)$$

Here, $\widehat{W}^{(k)}$ is the *passive form* [2], [12] of the generator $W^{(k)}$. Although the *active form* $W^{(k)}$ is nonunitary in general, it cooperates with its passive form to produce the isometry-like

[11] In [21], J. and P. Bertrand also consider affine smoothing of the affine Wigner distributions to obtain positive TSD's.

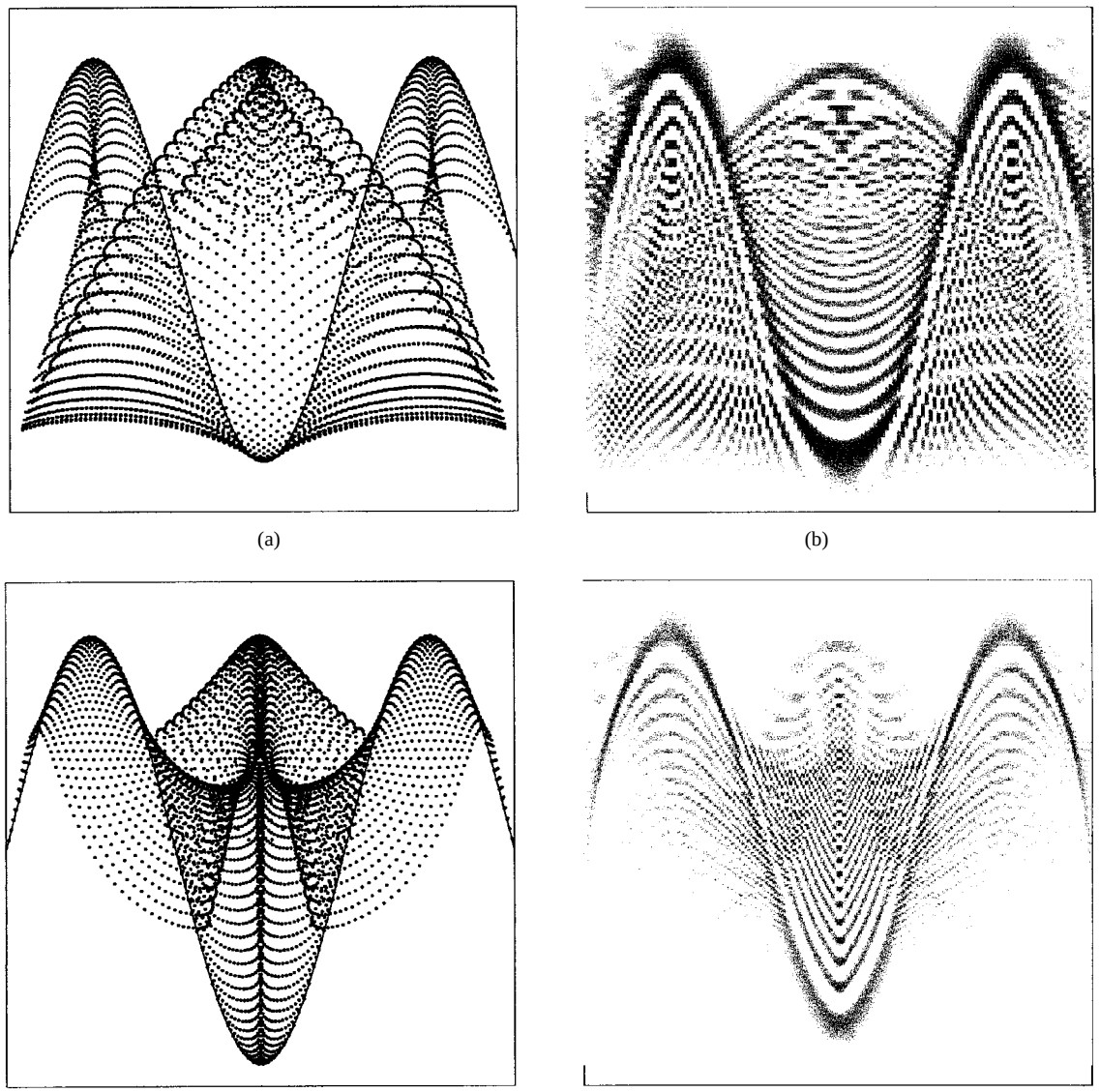

(a) (b) (c) (d)

Fig. 6. Accurate approximation of affine Wigner distributions using pseudo affine Wigner distributions. Horizontal axis corresponds to time and vertical axis to frequency. The test signal x is a sinusoidal frequency modulation $x(t) = \exp[-i\, f_m^{-1}\, \cos(2\pi f_m t)]$. (a) Predicted locus of the true distribution $P_x^{(-5)}$ as determined using the geometric construction rules of [4] and [5]. (b) Approximate affine Wigner distribution $\widetilde{P}_x^{(-5)}$ computed as in (28) using a narrowband wavelet of $Q = 130$. (c) Predicted locus of the true distribution $P_x^{(5)}$. (d) Approximate affine Wigner distribution $\widetilde{P}_x^{(5)}$.

relation [2]

$$\iint_0^\infty W_x^{(k)}(t,f)\, \widehat{W}_y^{(k)}(t,f)\, df\, dt = \left| \int x(u)\, y^*(u)\, du \right|^2. \tag{36}$$

In this case, (30) simplifies to

$$|D_x(t,f)|^2 = \iint_0^\infty W_x^{(k)}(\tau,\nu)\, \widehat{W}_\psi^{(k)}\left[f(\tau - t), \frac{\nu}{f} \right] d\nu\, d\tau \tag{37}$$

which is a natural generalization of (34).

V. Conclusions

Although the affine Wigner distributions have many attractive properties, interference terms and lack of efficient implementations have limited their impact on time-varying signal analysis. By overcoming these limitations, the pseudo and smoothed pseudo affine Wigner distributions should open up new application areas to these powerful tools. In particular, the flexible wavelet-based structure underlying these new TSD's allows a continuous transition in smoothing between affine Wigner distributions and scalograms. Moreover, to tune the pseudo affine Wigner distributions to the local characteristics of the signal, we can adapt the wavelet ψ in the sliding algorithm using the techniques of [22].

The introduction of alternative generators for the affine class of TSD's simplifies the kernel formulation of the pseudo affine Wigner distributions. In addition, the concept of alternative generators could aid in the analysis and design of new affine distributions matched to particular classes of signals.

APPENDIX A
PSEUDO AFFINE WIGNER KERNELS

We will derive an affine Wigner generator $W^{(k)}$ for use in (30) that provides a closed-form expression for the kernel $\Pi^{(k)}$ corresponding to the smoothed pseudo affine Wigner distribution $\widetilde{P}^{(k)}$.

Plugging the frequency-domain formulation of the wavelet transform (12) into (29) followed by the change of variables

$$\begin{cases} \nu = \theta\lambda_k(u) \\ \nu' = \theta\lambda_k(-u) \\ \text{with Jacobian } \dfrac{\partial(\nu,\nu')}{\partial(\theta,u)} = \theta\lambda_k(u)\lambda_k(-u) \end{cases} \tag{38}$$

leads to

$$\begin{aligned} \widetilde{P}_x^{(k)}(t,f) = \iiint_0^\infty & G(u)\,\mu_k(u)\,\frac{\nu}{f}\,\frac{\lambda_k(v)\lambda_k(-v)}{\lambda_k(u)\lambda_k(-u)} \\ & \times X[\nu\lambda_k(v)]X^*[\nu\lambda_k(-v)]\Psi^*\left[\frac{\nu\lambda_k(v)}{f\lambda_k(u)}\right] \\ & \times \Psi\left[\frac{\nu\lambda_k(-v)}{f\lambda_k(-u)}\right] e^{-i2\pi\nu t\xi_k(v)}\,d\nu\,dv\,du. \end{aligned} \tag{39}$$

Now, using the identity

$$X[\nu\lambda_k(v)]\,X^*[\nu\lambda_k(-v)] = \int W_x^{(k)}(\tau,\nu)\,e^{i2\pi\nu\tau\xi_k(v)}\,d\tau \tag{40}$$

for the natural generator (32), we obtain (41), shown at the bottom of the page, which is of the form (30) with an affine transformed version of the kernel (33) in square brackets. □

APPENDIX B
UNITARY GENERATORS

We will show that the only generator of the form (32) that is unitary is the usual Wigner distribution $W = P^{(2)}$ from (4). In a unitary affine Wigner distribution, the function μ_k takes on the special form [2]

$$\mu_k^U(u) = \left\{\lambda_k(u)\,\lambda_k(-u)\,\frac{d}{du}[\lambda_k(u) - \lambda_k(-u)]\right\}^{1/2}. \tag{42}$$

On the other hand, affine Wigner generators of the form (32) are characterized by

$$\mu_k^G(u) = \frac{d}{du}\,\xi_k(u) \tag{43}$$

$$= \frac{d}{du}\,[\lambda_k(u) - \lambda_k(-u)]. \tag{44}$$

In both cases, the function λ_k must also possess the symmetry property (17).

Solution of the differential equation $\mu_k^U = \mu_k^G$ or, after simplification,

$$\lambda_k(u)\,\lambda_k(-u) = \frac{d}{du}[\lambda_k(u) - \lambda_k(-u)] \tag{45}$$

subject to the constraint (17) will characterize the set of affine Wigner generators of the form (32) that are unitary.

By decomposing the function $\lambda_k(u)$ into the sum of its even part $e(u)$ and odd part $o(u)$, we can rewrite (45) as

$$e^2(u) = o^2(u) + 2\frac{d}{du}o(u) \tag{46}$$

and rewrite (17) as

$$e(u) - o(u) = e^{-u}\,[e(u) + o(u)] \tag{47}$$

or, equivalently, as

$$o(u) = e(u)\,\tanh\frac{u}{2}. \tag{48}$$

If we substitute (48) into (46) and solve for $o(u)$, we obtain

$$o^2(u) = \tanh^2\left(\frac{u}{2}\right)\left[o^2(u) + 2\frac{d}{du}o(u)\right] \tag{49}$$

or, equivalently

$$\frac{d}{du}\left[\frac{1}{o(u)}\right] = \frac{\tanh^2\dfrac{u}{2} - 1}{2\tanh^2\dfrac{u}{2}}. \tag{50}$$

Using the change of variables $x = \tanh(u/2)$, the unique solution of this equation is

$$o(u) = \tanh\frac{u}{2} \tag{51}$$

which implies, from (48), that $e(u) = 1$.

Thus, any affine Wigner distribution that is both unitary and a generator of the form (32) must be based on a λ_k function of the form

$$\lambda_k(u) = 1 + \tanh\frac{u}{2} \tag{52}$$

which is true only for $k = 2$ (Wigner distribution). □

$$\begin{aligned} \widetilde{P}_x^{(k)}(t,f) = \iint_0^\infty W_x^{(k)}(\tau,\nu) \Bigg[& \frac{\nu}{f}\iint G(u)\,\mu(u)\,\frac{\lambda_k(v)\lambda_k(-v)}{\lambda_k(u)\lambda_k(-u)} \\ & \times \Psi\left[\frac{\nu}{f}\,\frac{\lambda_k(v)}{\lambda_k(u)}\right]\Psi^*\left[\frac{\nu}{f}\,\frac{\lambda_k(-v)}{\lambda_k(-u)}\right] e^{i2\pi(\nu/f)f(\tau-t)\xi_k(v)}\,du\,dv\Bigg]\,d\nu\,d\tau \end{aligned} \tag{41}$$

APPENDIX C
TIME-LOCALIZED GENERATORS

Using methods similar to those in Appendix B, we will demonstrate that the only generator of the form (32) that is time localized is the active Unterberger distribution $P^{(-1)}$ with $\mu_{-1}(u) = \cosh(u/2)$ [2], [12]. In a time-localized affine Wigner distribution, the function μ_k takes on the special form [2], [17]

$$\mu_k^L(u) = [\lambda_k(u)\,\lambda_k(-u)]^{1/2}\,\frac{d}{du}[\lambda_k(u) - \lambda_k(-u)]. \quad (53)$$

Solution of the differential equation $\mu_k^L = \mu_k^G$ or, after simplification,

$$\lambda_k(u)\,\lambda_k(-u) = 1 \quad (54)$$

subject to (17) will characterize the set of affine Wigner distributions that are simultaneously time localized and natural generators. Imposing (17) yields the unique solution to (54)

$$\lambda_k(u) = e^{u/2} \quad (55)$$

which holds only for $k = -1$ (active form of the Unterberger distribution). □

ACKNOWLEDGMENT

The authors would like to thank P. Flandrin for setting us on the path to the pseudo affine Wigner distributions. They also thank J. and P. Bertrand and the reviewers for their insightful comments and suggestions.

REFERENCES

[1] L. Cohen, *Time-Frequency Analysis.* Englewood Cliffs, NJ: Prentice-Hall, 1995.
[2] J. Bertrand and P. Bertrand, "A class of affine Wigner functions with extended covariance properties," *J. Math. Phys.*, vol. 33, pp. 2515–2527, July 1992.
[3] O. Rioul and P. Flandrin, "Time-scale energy distributions: A general class extending wavelet transforms," *IEEE Trans. Signal Processing*, vol. 40, pp. 1746–1757, July 1992.
[4] P. Flandrin and P. Gonçalvès, "Geometry of affine distributions," in *IEEE Int. Symp. Time-Freq. Time-Scale Anal.*, Philadelphia, PA, 1994, pp. 80–83.
[5] ——, "Geometry of affine time-frequency distributions," *Applied Computat. Harmonic Anal.*, vol. 3, pp. 10–39, Jan. 1996.
[6] P. Flandrin, *Temps-Fréquence.* Paris, France: Hermès, 1993.
[7] T. A. C. M. Claasen and W. F. G. Mecklenbräuker, "The Wigner distribution—A tool for time-frequency signal analysis—Part I: Continuous-time signals," *Philips J. Res.*, vol. 35, no. 3, pp. 217–250, 1980.
[8] L. Stanković, "A method for time-frequency analysis," *IEEE Trans. Signal Processing*, vol. 42, pp. 225–229, Jan. 1994.
[9] J. Bertrand and P. Bertrand, "Time-frequency representations of broad-band signals," in *Proc. IEEE Int. Conf. Acoust., Speech, Signal Process., ICASSP*, New York, NY, 1988, pp. 2196–2199.
[10] P. Flandrin, "Sur une classe générale d'extensions affines de la distribution de Wigner-Ville," in *Proc. 13ème Colloque GRETSI*, Juan Les Pins, France, Sept. 1991, pp. 17–20.
[11] R. G. Shenoy and T. W. Parks, "Wide-band ambiguity functions and affine Wigner distributions," *Signal Process.*, vol. 41, no. 3, pp. 339–363, 1995.
[12] A. Unterberger, "The calculus of pseudo-differential operators of Fuchs type," *Commun. Part. Diff. Equations*, vol. 9, pp. 1179–1236, 1983.
[13] T. Posch, "Wavelet transforms and time-frequency distributions," in *Proc. SPIE Int. Soc. Opt. Eng.*, 1988, vol. 1152, pp. 477–482.
[14] J. Bertrand and P. Bertrand, "Some practical aspects of the affine time-frequency distributions," in *Proc. 13ème Colloque GRETSI*, Juan Les Pins, France, Sept. 1991.
[15] P. Gonçalvès and R. Baraniuk, "Pseudo affine Wigner distributions," in *Proc. IEEE Int. Conf. Acoust., Speech Signal Process., ICASSP*, Atlanta, GA, 1996.
[16] ——, "A pseudo Bertrand distribution for time-scale analysis," *IEEE Signal Processing Lett.*, vol. 3, pp. 82–84, Mar. 1996.
[17] J. P. Ovarlez, J. Bertrand, and P. Bertrand, "Computation of affine time-frequency distributions using the fast Mellin transform," in *Proc. IEEE Int. Conf. Acoust., Speech, Signal Process.—ICASSP*, San Francisco, CA, 1992, pp. V117–V120.
[18] D. L. Jones and R. G. Baraniuk, "Efficient approximation of continuous wavelet transforms," *Inst. Elect. Eng. Electron. Lett.*, vol. 27, pp. 748–750, Apr. 25, 1991.
[19] P. Flandrin and P. Gonçalvès, "From wavelets to time-scale energy distributions," in *Recent Advances in Wavelet Analysis*, G. W. L. L. Schumaker, Ed. San Diego, CA: Academic, 1994, pp. 309–334.
[20] F. Hlawatsch, A. Papandreou, and G. F. Boudreaux-Bartels, "Regularity and unitarity of affine and hyperbolic time-frequency representations," in *Proc. IEEE Int. Conf. Acoust., Speech, Signal Process. ICASSP*, Minneapolis, MN, 1993, pp. III.245–III.248.
[21] J. Bertrand and P. Bertrand, "Affine time-frequency distributions," in *Time-Frequency Signal Analysis—Methods and Applications*, B. Boashash, Ed. Melbourne, Australia: Longman–Cheshire, 1992, pp. 118–140.
[22] D. L. Jones and R. G. Baraniuk, "A simple scheme for adapting time-frequency representations," *IEEE Trans. Signal Processing*, vol. 42, pp. 3530–3535, Dec. 1994.

Paulo Gonçalvès (S'94–M'96) graduated from the Signal Processing Department of ICPI, Lyon, France, and received the Masters (DEA) and Ph.D. degrees in signal processing from the Institut National Polytechnique, Grenoble, France, in 1990 and 1993.

While working toward the Ph.D. degree, he was with Ecole Normale Supérieure, Lyon. In 1994, he was a Postdoctoral Fellow at Rice University, Houston, TX. He then joined the research group FRACTALES at INRIA, Rocquencourt, France, where he is currently a Chargé de Recherche. His research interests are in the application of affine time–frequency representations to multifractal signals and image processing.

Richard G. Baraniuk (M'93–SM'97) received the B.Sc. degree in 1987 from the University of Manitoba, Winnipeg, Man., Canada, the M.Sc. degree in 1988 from the University of Wisconsin, Madison, and the Ph.D. degree in 1992 from the University of Illinois, Urbana–Champaign, all in electrical engineering.

In 1986, he was a Research Engineer with Omron Tateisi Electronics, Kyoto, Japan. After spending 1992 and 1993 with the Signal Processing Laboratory of Ecole Normale Supérieure, Lyon, France, he joined Rice University, Houston, TX, where he is currently an Associate Professor of Electrical and Computer Engineering. His research interests lie in the area of signal and image processing and include wavelet theory and time–frequency analysis.

Dr. Baraniuk received a NATO Postdoctoral Fellowship from NSERC in 1992, a National Young Investigator Award from the National Science Foundation in 1994, and a Young Investigator Award from the Office of Naval Research in 1995.